Preprint
UCRL-JC-139404

Direct Comparison Between Modeling and Experiment: An α-Fe Ion Implantation Study

J. Marian, B.D. Wirth, J.M. Perlado, T. Diaz de la Rubia, R. Schäublin, D. Lodi, M. Hernández, G. de Diego, R. Stoller

This article was submitted to Materials Research Society Fall 2000 Symposium R, Boston, MA, November 27 – December 1, 2000

January 25, 2001

U.S. Department of Energy

Lawrence Livermore National Laboratory

This work was performed under the auspices of the United States Department of Energy by the University of California, Lawrence Livermore National Laboratory under contract No. W-7405-Eng-48.

DIRECT COMPARISON BETWEEN MODELING AND EXPERIMENT: AN α-Fe ION IMPLANTATION STUDY

Jaime Marian[1], Brian D. Wirth[1], J. Manuel Perlado[2], T. Diaz de la Rubia[1], Robin Schäublin[3], Dario Lodi[2], Mercedes Hernández[4], Gonzalo de Diego[4], Dolores G. Briceño and Roger E. Stoller[5]

[1]Chemistry and Materials Science Directorate, Lawrence Livermore National Laboratory, P. O. Box 808, L-353, Livermore, CA 94550, U.S.A.

[2]Instituto de Fusión Nuclear, Universidad Politécnica de Madrid, C/ José Gutiérrez Abascal, 2; Madrid 28006, SPAIN

[3]CRPP, Fusion Technology-Materials, Ecole Polytechnique Fédérale de Lausanne, CK-5232, Villigen PSI, SWITZERLAND

[4]Departamento de Fisión Nuclear, CIEMAT, Avda. Complutense, 22; Madrid 28040, SPAIN

[5]Metals and Ceramics Division, Oak Ridge National Laboratory, P. O. Box 2008, Oak Ridge, TN 37831-6376, U.S.A.

ABSTRACT

Advances in computational capability and modeling techniques, as well as improvements in experimental characterization methods offer the possibility of directly comparing modeling and experiment investigations of irradiation effects in metals. As part of a collaboration among the *Instituto de Fusión Nuclear* (DENIM), *Lawrence Livermore National Laboratory* (LLNL) and CIEMAT, single and polycrystalline α-Fe samples have been irradiated with 150 keV Fe-ions to doses up to several dpa. The irradiated microstructure is to be examined with both transmission electron microscopy (TEM) and positron annihilation spectroscopy (PAS). Concurrently, we have modeled the damage accumulation in Fe under these irradiation conditions using a combination of molecular dynamics (MD) and kinetic Monte Carlo (KMC). We aim to make direct comparison between the simulation results and the experiments by simulating TEM images and estimating positron lifetimes for the predicted microstructures. While the identity of the matrix defect features cannot be determined from TEM observations alone, we propose that both large self-interstitial loops, trapped at impurities within the material, and small, spherical nanovoids form.

INTRODUCTION

With the development of modern computer capabilities, efficient algorithms and realistic interatomic potentials and parametrizations, atomistic simulation techniques including *ab initio*, tight-binding and classical molecular dynamics (MD) have reached a degree of accuracy and resolution sufficient to reliably provide materials properties at the atomic level. However, inherent spatial and temporal limitations of MD confines its applicability for radiation damage studies to primary defect production and selected defect transport properties. Modeling damage accumulation and microstructural evolution resulting from particle irradiation requires the use of kinetic Monte Carlo (KMC) or kinetic rate theory approaches, which can effectively incorporate MD property databases. Ultimately, predictions of microstructural evolution can be coupled to dislocation dynamics models or dislocation theory to provide predictions of the resulting mechanical property changes. When coupled self-consistently and in a sequential manner,

multiscale modeling of radiation damage can provide mechanical property change predictions such as yield strength or transition temperature shifts useful for engineering applications. On the other hand, experimental validation represents an important component in the development of multiscale models. Yet, comparisons between modeling and experimental characterization of radiation damage are difficult to make and often qualitative at best. Recently, Odette has proposed the idea of a computational microscope [1], i.e. using computational models to directly simulate experimental characterization techniques and to improve comparisons between modeling predictions and experiment. Thus, a custom irradiation experiment has been designed to approximate the conditions that can be best reproduced with the current implementations of MD and KMC codes. Further, the modeling predictions will be used to simulate the TEM and positron annihilation analysis and compare with the experimentally characterized radiation damaged microstructures. The experiments, conducted by CIEMAT, are presently under way and in this paper, we present the first results of the combined MD/KMC approach carried out at LLNL and DENIM to reproduce the experimental conditions.

The starting point of these simulations is the primary damage state, that is, the spatially correlated locations of vacancies, interstitials and their clusters, obtained from MD simulations of displacement cascades. MD currently simulates times on the order of 100 picoseconds with a few nm of spatial resolution. KMC calculations track the size and number density of point defects and defect clusters that form following the introduction of a primary knock-on atom (PKA) in the material, giving measurements of such quantities as the fraction of freely migrating defects as well as the number, size and position of defect clusters, such as loops and nanovoids in the system. The latest, most efficient versions of the BigMac KMC [2] code now allow simulation times of the order of tens of seconds. The outcome of this multiscale approach, i.e. the spatial position and number of defect clusters, can be used as input into techniques to calculate the observed TEM and positron lifetime experimental signals. In this paper we report the first results simulating the experimental conditions up to doses of 0.66 dpa.

EXPERIMENTAL AND MODELING

Experimental conditions

Two sets of experiments involving high purity Fe crystals have been performed, one at a high dose rate (~10^{13} $cm^{-2}s^{-1}$; 0.051 dpa/s) and long irradiation time (5 min; ~15.3 dpa) and another one at a lower dose rate (~10^{12} $cm^{-2}s^{-1}$; 0.0051 dpa/s) and short irradiation time (0.3 s; ~0.0015 dpa), to evaluate the effect of dose rate and total accumulated dose in the system. In this paper we focus only on the high-dose case. The irradiation conditions of the TEM foils relevant to the simulations are dose =10^{16} ion·cm^{-2} (15.3 dpa), dose rate =3.34×10^{13} ion·cm^{-2}·s^{-1} (0.051 dpa/s), temperature =300 K and PKA energy =150 keV. In the simulations performed to date, we have reached ~0.6 dpa, which represents an extension of previous damage accumulation simulations to higher dose [2-4].

Simulation methodology

A combined multiscale TRIM/MD/KMC approach was used. TRIM provides the recoil energy and penetration distributions derived from a 150-keV ion beam on Fe. These recoil energy distributions, in conjunction with a MD database of displacement cascades at energies between 0.5 to 50 keV are used to construct a cascade defect production library. This library is the basis for simulating the effect of each ion impact in the KMC damage accumulation model. MD is also used to supplement the understanding of defect binding and migration energies and diffusion coefficients. Thus, input to the Monte Carlo calculation comes mainly from MD in the form of defect cluster energetics and collision cascade simulations. The KMC BigMac code [2] tracks the evolution of all defects at the pertinent dose rate as a function of increasing dose. Simulations were performed in a 100×100×100 nm box where free surfaces and dislocations act as first-order defect sinks. Simulations have been performed for both pure Fe and Fe containing 20 and 100 atomic parts per million (appm) of interstitial impurities. These generic trapping sites represent immobile, (octahedral) interstitial impurity atoms such as C, O or N, with an assumed binding energy of 1.0 eV to both SIA and SIA clusters. This value has not yet been rigorously calculated in the literature and serves only as a first estimate for our simulations. Additional details on the defect energetics employed, model assumptions and other calculation details can be found elsewhere [5].

BigMac provides the number and size of all possible defect clusters in the simulation box as a function of time (dose). Using the primary damage state from the displacement cascades discussed above as input data, we have computed the rate of damage accumulation as a function of dose. However, due to the comparative nature of this work, it is useful to calculate the number density of 'visible' clusters in terms of TEM resolution limits, that is, the number of defect clusters larger than a minimum size resolvable by TEM. Depending on the type of defect, this magnitude can be approximated as the diameter of planar prismatic interstitial loops or spherical vacancy loops. In our calculation we have taken a conservative TEM resolution of 2 nm as this is a value commonly quoted in the literature [6, 7] as well as the reported TEM resolution at CIEMAT.

As noted above, interstitial clusters generated directly by displacement cascades form loops that are glissile and highly mobile. These loops are of $\langle 111 \rangle \{110\}$ slip geometry, the faces of the glide prism lying on {110} planes. The prism contour can have various shapes, the most stable one generally being hexagonal and not necessarily planar in structure [8]. However, for the sake of simplicity, in our model self-interstitial atom (SIA) clusters are approximated as planar loops of circular shape and, hence, based on, geometric arguments, 67 self-interstitials correspond to the minimum TEM resolvable loop, with a diameter of 2 nm. On the other hand, while vacancy loops have been observed in some circumstances of ion-irradiated Fe at high doses [9], the majority of evidence suggests that vacancy clusters maintain a roughly spherical, three-dimensional morphology [3, 10, 11]. Therefore, vacancy clusters in our model are seen as small 3D nanovoids rather than as faulted loops and, accordingly, 178 vacancies constitute the minimum TEM visible feature.

RESULTS

Figure 1 (a) shows the evolution with dose (time) of the total and visible SIA cluster densities for impurity concentrations of 20 and 100 appm. In pure Fe, e.g. without interstitial impurities, no self-interstitial clusters remain, indicating that, in the absence of trapping sites, all SIAs and SIA clusters either rapidly migrate to sinks or recombine. In the two impurity trapping cases investigated (20 and 100 appm), defect cluster saturation is reached at about 0.1 dpa where roughly 87 and 80% of the impurities present in the material hold SIA clusters respectively. The remaining 'free' impurities are mainly those located close to the rear face of the simulation box where damage penetration is not as intense.

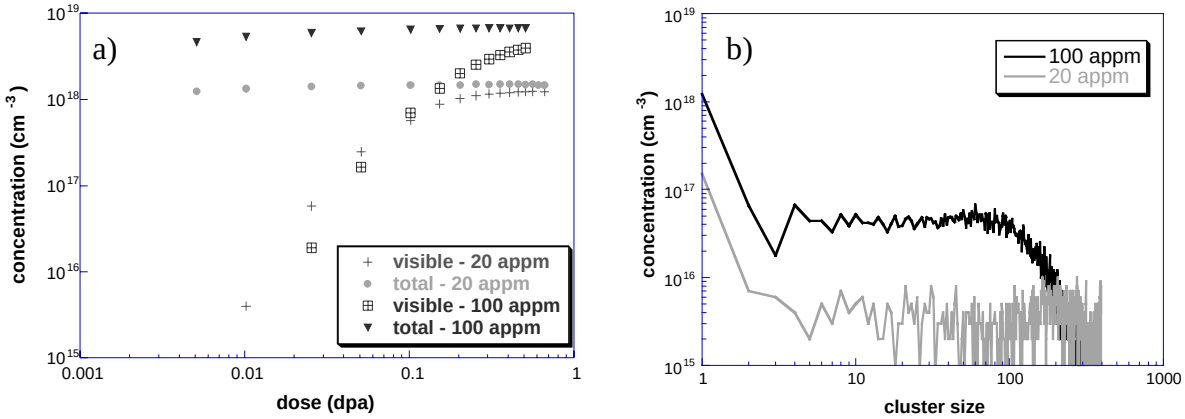

Figure 1. *(a) Evolution with dose of the number density of total and visible SIA clusters for 20 and 100 appm. For 0 appm all SIAs and SIA clusters disappear at sinks. (b) Interstitial size distribution for the maximum accumulated dose in each case.*

With increasing dose, the trapped SIA clusters are biased nuclei for SIA (and SIA cluster) absorption and grow to observable sizes. As shown in Figure 1 (a), the concentration of observable SIA loops asymptotically approaches the total cluster density. The SIA cluster size distribution can be seen in figure 1 (b) (at 0.66 dpa for 20 appm and 0.51 for 100 appm). Besides the difference in magnitude between both curves, the 20-appm distribution presents a higher proportion of very large clusters (N >200, d >3.5 nm). We ascribe this difference to the fact that a similar SIA flux (determined by cascade introduction rate) distributes over a much more dilute impurity density. Of course, losses to free surfaces and extended sinks will also be greater as a consequence of a less concentrated trapped interstitial cluster density but the overall size distribution shifts upward towards numbers between 200 and 400.

Figure 2 (a) shows the evolution with dose of the free vacancy and vacancy cluster concentrations for the three impurity cases considered. Both free vacancies and clusters follow the same pattern in accordance with the low temperature, high sink density behavior pointed out by Sizmann [12]. Saturation in this case occurs much later than in the interstitial case (at about 1 dpa of accumulated dose) which is a consequence of the difference in mobility between both species. Also, it can be seen that there are no significant differences among the three impurity cases considered, especially at high doses, which leads us to believe that mutual vacancy-interstitial recombination occurs within the cascade volume before SIAs 'see' any impurities and, therefore, is only dependent on dose and dose rate.

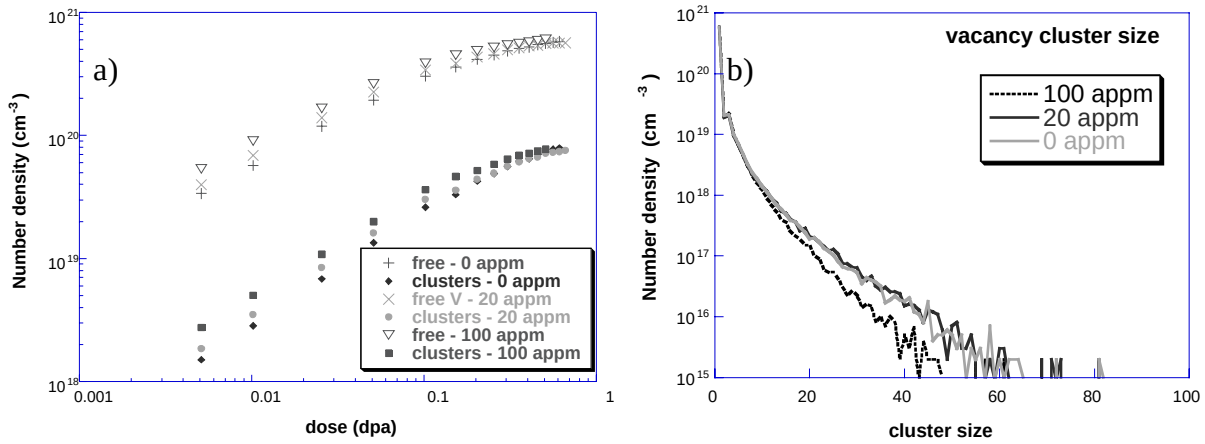

Figure 2. *(a) Evolution with dose of the number density of free vacancies and vacancy clusters and (b) vacancy cluster size distribution for 0, 20 and 100 appm.*

Figure 2 (b) shows the vacancy cluster size distribution at the maximum accumulated doses in each case (0.66 dpa for 0 and 20 appm and 0.51 dpa for 100 appm). The largest clusters observed have 84 vacancies, well below the required 178 for a nanovoid to be observable by TEM. However, the large number density of vacancy-type defects, particularly single vacancies, suggest that there will appear a marked increase in the intensity of the corresponding positron lifetime distribution. The average size of the vacancy clusters has been observed to gradually approach or fluctuate around 5 with dose. Since vacancy mobility at 300 K is very low, these clusters are mainly formed by direct combination of vacancies within the interaction volume of each other (r =0.287 nm). These events are produced directly by displacement cascades rather than by vacancy diffusion and explain the differences between the vacancy and self-interstitial size and number distributions.

As mentioned before, TEM image simulation can be used to calculate images for comparison with experimental micrographs. They can indicate if the type of defects observed is the same in both cases and can also be used to determine the experimental conditions under which experimental images were taken. Analogously, positron lifetime calculations can provide insight into the size, shape and number density of the otherwise non-(TEM) visible vacancy clusters. Work is under way to perform these calculations, specifically TEM image simulation of perfect (hexagonal) SIA loops lying on (110) and (111) planes with Burgers vector $\mathbf{b}=(a_o/2)\langle 111\rangle$ and positron lifetimes of small (N =5) vacancy voids.

CONCLUSIONS

Preliminary results of a multiscale modeling simulation of damage accumulation for Fe irradiated with 150 keV Fe ions are presented. In this model, SIA clusters trapped at interstitial impurities serve as nuclei and grow into self-interstitial loops which we predict will be visible in TEM examinations. Increasing interstitial impurity content appears to have little effect on the number and size distributions of vacancy cluster defects, which are assumed to be three-dimensional nanovoids and are expected to result in a significant increase in positron lifetime values. These modeling results will be used to simulate predicted TEM images and positron lifetime values for direct comparisons with experimental characterization of a custom ion-irradiation experiment, to be performed by CIEMAT.

ACKNOWLEDGMENTS

This work has been performed under the auspices of the US Dept. Of Energy at LLNL under contract W-7405-Eng-48 and within the CSN-UNESA PCI (Venus Project) under contract P970530432.

REFERENCES

[1] G.R. Odette, in *Microstructure of Irradiated Materials*, edited by I.M. Robertson, L.E. Rehn, S.J. Zinkle, and W.J. Phythian (Mater. Res. Soc. Symp. Proc. **373**, Pittsburgh, Pa, 1995) p. 137.
[2] M. J. Caturla, N. Soneda, E. Alonso, B. D. Wirth, T. Diaz de la Rubia and J. M. Perlado, J. Nucl. Mat **276**, 13 (2000)
[3] N. Soneda and T. Diaz de la Rubia, Phil. Mag. A **78**, 995 (1998)
[4] E. Alonso, M. J. Caturla, T. Diaz de la Rubia and J. M. Perlado, J. Nucl. Mat **276**, 221 (2000)
[5] J. Marian, B. D. Wirth, J. M. Perlado, T. Diaz de la Rubia, G. de Diego, M. Hernández and D. G. Briceño, talk delivered at: ASTM *20th International Symposium on Effects of Radiation on Materials*, Williamsburg, VA, 5-8 June 2000, unpublished
[6] Y. Dai and M. Victoria in: *Microstructural Evolution under Irradiation*, edited by I. M. Robertson, G. S. Was, L. W. Hobbs and T. Diaz de la Rubia (Mater. Res. Soc. Proc. **439**, Warrendale, PA, 1997) p. 319
[7] B. N. Singh and S. J. Zinkle, J. Nucl. Mat **206**, 212 (1993)
[8] B. D. Wirth, G. R. Odette, D. Maroudas and G. E. Lucas, J. Nucl. Mat **276**, 33 (2000)
[9] M. L. Jenkins, C. A. English and B. L. Eyre, Phil. Mag. A **38**, 97 (1978).
[10] G. R. Odette and B. D. Wirth, J. Nucl. Mat **251**, 157 (1997).
[11] M. Eldrup and B. N. Singh, J. Nucl. Mat **276**, 269 (2000).
[12] R. Sizmann, J. Nucl. Mat **69-70**, 386 (1968)